한국소성가공학회 '97추계학술대회 논문집 pp.158～163

# Optimization of the Tool Geometry of Plane Strain Punch Stretching Test

*Dongho Ha and **Youngsuk Kim
* Graduate School, Kyungpook National University
**Kyungpook National University

# 평면변형률 장출 실험용 금형의 최적설계

*하동호, **김영석
*경북대학교 기계공학부 대학원
**경북대학교 기계공학부

**Abstract**

In this paper the tool geometry of the PSS test were optimized in order to assure the reliability of the test. Considering many factors for optimization of the tool geometry, computer-simulation technique using three-dimensional finite element method(FEM) was used. Three design variables - the punch length, punch crown and punch corner radius - are chosen to be optimized according to the Taguchi's experiment technique with the $L_9$ orthogonal array. The optimum condition to ensure the plane strain mode over the overall area of the specimen was clarified. Moreover the simulation results are confirmed by experiment.

Key word : Plane strain punch strtching test, Taguchi method, orthogonal array

## 1. Introduction

Recently, a new simple test method called plane strain stretching (PSS) test has been developed and used successfully in the evaluation of the press formability of automotive steel sheets. The prototype tool geometry of the original PSS test was determined by the repeated experimentations. In the conventional PSS test with high punch speed, 300mm/min, fracture occurs cross the specimen concurrently both at the center of symmetry and near the punch corner area. However, in a special testing condition of relatively low punch speed the fracture seems to occur nearby punch corner in advance and successively propagates to the center of symmetry of specimen. This is due to excessive local bending deformation exceeding the material stretchability at the punch corner before reaching material stretchability in the plane strain mode over the overall area of the specimen. Therefore the original tool geometry of the PSS test may result in the underestimation of LPH value. It seems to decrease a reliability in evaluation method on stamping formability of sheet material. Therefore it is a prerequisite to ensure an optimized tool geometry which yields more stable and better reproducibility on PSS test.

In this study, the optimization of tool geometry of PSS test was performed to overcome the shortcut of the original tool shape by using PAM_STAMP code[11], a commercial finite element method package. Here, three design variables -the punch length, punch crown and punch corner radius- are chosen to be optimized according to the Taguchi's experiment technique. Also, the simulation results were compared with those of experiment.

## 2. Finite element simulation

Fig. 1(a),(b) shows schematics of tool set up geometry -punch, blank holder and die- under PSS testing and tested specimen of PSS test. Fig. 2 shows the finite element model of PAM-STAMP for the PSS test process. Here, due to the symmetry of deformation, FE simulation with plane stress assumption was done for a quarter of the specimens. Table 1 shows the mechanical properties of the specimen, commercial quality steel sheet(CQ).

## 3. Taguchi's orthogonal array

In the PSS test of original tool geometry with relatively low punch speed, a fracture seems to occur nearby punch corner in advance and propagate to the center of symmetry of specimen because the major strain at the punch corner is larger than that of the center of symmetry of specimen. This stems from the difference of the magnitude in major strain between at the punch corner and the center of the symmetry of the specimen. If the difference of major strain variation along punch stroke, $\Delta\varepsilon_1 = \varepsilon_{1cp} - \varepsilon_{1cs}$, between at the punch corner, $\varepsilon_{1cp}$, and the center of the symmetry, $\varepsilon_{1cs}$, as shown in Fig.3 were minimized by changing the tool geometry, we can conclude that the tool geometry is optimized. Therefore the difference of major strain variation along punch stroke between two area was chosen as a quality characteristic in tool geometry optimization problem of the PSS test. By using the quality characteristic, this problem becomes the smaller-the-better type problem in the Taguchi method, which means that the smaller is the difference of major strain, the better is PSS test. The signal-to-noise(S/N) ratio, $\eta_i$, for experiment $i$ is given as follows.

$$\eta_i(dB) = -10\log_{10}(\Delta\varepsilon_1^2), \qquad (1)$$

The maximizing procedure of the S/N ratio minimizes the difference of major strain between two area, so that the best condition of PSS experiment can be obtained by maximizing $\eta_i$. The factors to be considered here to establish their effects on PSS experiment are the punch crown(h) defined by ellipsoidal shape, the punch corner radius(Rp) and punch length($L_1$, $L_2$). Fig.4 shows the definition of these factors. Here the punch crown of ellipsoidal shape along the punch length direction was introduced to reduce the tendency of in-advance fracture at the punch corner. These three factors and their selected levels being listed in Table 2.

## 4. Results and discussion

Table 3 shows the results of matrix experiment along the $L_9$ orthogonal array. PAM_STAMP simulation according to the matrix experiment will clarify the relative magnitude of the effect of each factor. Moreover, analysis of mean(ANOM) and analysis of variance(ANOVA) for the quality characteristic will afford a better understanding of the individual effect of each other.

Fig.5 shows the variations of thickness measured near highly strained elements versus punch stroke for the case of No. 1. Generally as the punch stroke increases, the thicknesses of the elements near highly strained area decrease rapidly due to stretching deformation. However, after failure occurred the stress acting on the area is released, thus there is no more thinning of these elements. The point indicating a drastic change of thickness variation corresponds to the calculated LPH value ($LPH_{cal}$) in FE simulation. At this $LPH_{cal}$ value we measured the major strain value, $\varepsilon_1$.

Fig.6 shows the major strain variations versus punch stroke at the center of symmetry and at the punch corner for the case of No. 1, which means the case of original punch geometry. Two major strain curves change differently with respect to punch stroke, moreover, the magnitude of increase of major strain at the punch corner is larger than that at the center of symmetry during punch stroke. From this result, it is certain that a fracture may occur in advance at the punch corner and subsequently propagate to the center of symmetry of specimen. There we overlap the measured strains of the experiment. It is clear that the experimental results showing some difference in the magnitude of major strain measured at two area provides a good comparison with the simulation ones.

The calculated results are summarized in Table 4. It is clear that a change of level of the punch crown parameter cause a large variation of the quality characteristic. The punch crown parameter is responsible for $(782.8/993.5)\times100=78.8\%$ of total sum of squares, which implies that this factor significantly affects the deformation mode of material, thus being one major control factor. However, the punch corner radius and punch length contribute only 15.8% and 5.4% to the total variation of $\eta$, respectively.

Results of ANOVA for PSS test simulation are presented in Fig.7, from which it can be concluded that the punch crown parameter affects mainly the plane strain deformation mode of material. Also when the punch crown and punch corner radius has a factor level 2, the fracture of the plane strain stretching occurs more stably. Therefore, from ANOM and Fig.7, the optimum conditions to successfully maintain a stable condition of PSS test could be selected as $A_2B_2C_3D_1$, which means H=3mm, $R_p$=6mm , $L_1$=72mm and $L_2$=70mm in Table 3. The S/N ratio for this selected optimum conditions, denoted by $\eta_{opt}$, is predicted as follows:

$$\eta_{opt} = m + (m_{A_2} - m) + (m_{B_2} - m) = 49.95(dB) \quad (2)$$

In this study, the optimum condition is consistent with the case of No. 5 in Taguchi's orthogonal array. Therefore we don't need any additional simulations to confirm the validity of these simulations and the prediction error is 6.55. This error is within 95%

confidence interval with $\pm 2\sigma = \pm 13.06$, thus the orthogonal array for PAM_STAMP simulation of this model is appropriate and the result is reliable. If the prediction error is outside the limit of $2\sigma$, it should be suspected that the model may not be adequate and the interactions between each factor should be considered.

Fig.8 shows major strain variation versus punch stroke at the center of symmetry and at the punch corner for the case of No. 5 which is the optimal condition. The two curves of variation of major strain with respect to punch stroke are almost coincident. This means that the fracture of plane strain stretching occurs at the same time between the punch corner and the center of symmetry of specimen. This tendency meets our goal to pursue. Also the variation of the major strains measured in experiment was added in the figure. Experimental results confirms the validity of the simulation ones.

Fig.9 shows the experimental results for the specimen of CQ material using (a) original punch geometry, and (b) optimized punch geometry of ellipsoidal shape. In the case of Fig.9(a), the fracture occurred near punch corner in-advance due to excessive bending effect and subsequently propagated toward the center. It agrees well with our prediction in Fig.6. Therefore, it is clear that the calculated deformation behaviors well simulate the deformation phenomena observed in experiments and also the predicted fracture locations agree with the experimental ones. In the case of Fig.9(b), which is with the optimized punch, the fracture occurred concurrently at the center of the specimen and the punch corner under plane strain stretching mode. This backs up our prediction in Fig.8.

## 5.Conclusion ABBREVIATION

### Reference

1. Ghosh,A.K., Hecker,S.S., and Keeler, S.P., : *Sheet metal forming and testing, Workability Testing Techniques*, G.E.Dieter ed., p.125-95. ASM, Metals Parks, OH (1984).

2. *LDH Committee/NADDRG* : Final report of the LDH Committee, May (1990).

3. Suh,Y.S., and Wagoner,R.H., : *Optimized design of tooling of the new formability test, Computer Application in Shaping & Forming of Materials*, M.Y.Demeri ed., TMS,, p.221-28 (1993).

4. Suh,Y.S., and Wagoner,R.H., : *Application of the finite-element method to a design of optimized tool geometry for the O.S.U. formability test*, JMEPEG, Vol. 5, p.489-499 (1996)

5. Saunders,F.I., and Wagoner,R.H., : *Finite element modelling of a new formability test, Computer Application in Shaping & Forming of Materials*, M.Y.Demeri ed., TMS, p.205-20 (1993).

6. Kim,Y.S., Park,K.C., and Nam,J.B., : Development of plane strain punch stretching test, *J. Korean Soc. Mech Engng*, Vol.7-5, p.1132-37 (1993).

7. Kim,Y.S., and Park,K.C., : Comparison of friction coefficients of sheet materials in various deformation modes, *J. Korean Soc. Tech. Plasticity*, Vol.3-1, p.51-62 (1994).

8. Kim,Y.S., and Park,K.C., : A plane strain punch stretching test for evaluating stamping formability of steel sheets; *Metal. Trans.*, Vol.25A-10, p.2199-205 (1994).

9. Kim,Y.S., and Park,C.D., : A numerical and experimantal study of deformation characteristics of the plane strain punch stretching test, *Metal. Trans.*, Vol.28A-8, p.1653-1659 (1997).

10. Yoshida,T, and Katayama,T, and Usuda,M, : Forming limit analysis of hemispherical punch stretching using three-dimensional finite element method, *Proc. 2nd Int. Conf. NUMISHEET'93*, p.219-28 (1993).

11. PAM-STAMP™ version 2.1, User's Manual, Pam System International, ESI-GROUP Software Product Company, (1996)

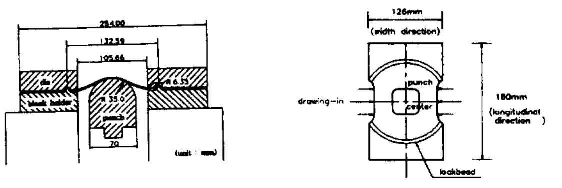

(a) (b)

Fig. 1 Schematics of (a) tool set up geometries and (b) the tested specimen of plane strain punch stretching test

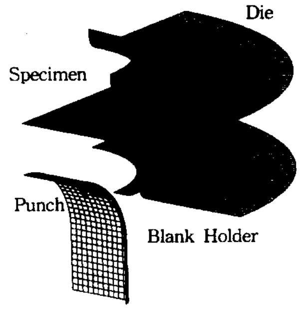


Fig.2 Finite element model

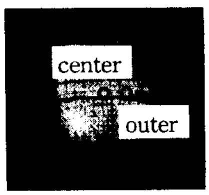


Fig.3 Measuring area of a major strain both at the punch corner and at the center of the symmetry of specimen

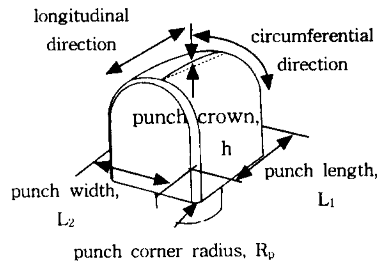


Fig 4 The definition of factors

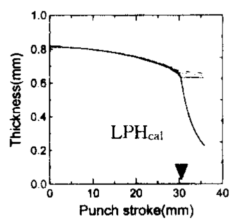


Fig.5 Variation of thickness versus punch stroke for the case of No. 1

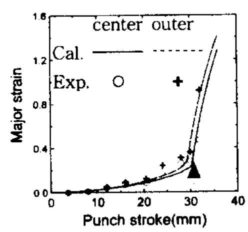


Fig.6 Variation of major strain versus punch stroke at the center of symmetry and at the punch corner for the case of No. 1

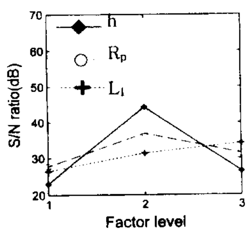


Fig.7 Showing the factor-effects on the variation of the S/N ratio

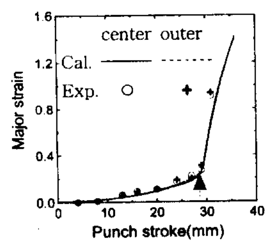


Fig.8 Variation of major strain versus punch stroke at the center of symmetry and at the punch corner for the case of No. 5

(a) (b)

Fig.9 Experimental results of the specimen of CQ material using (a) original punch geometry, and (b) optimized punch geometry of ellipsoidal shape

Table 1 Mechanical properties of tested material

| Material | t(mm) | K(MPa) | $\varepsilon_o$ | n | $R_n$ |
|---|---|---|---|---|---|
| CQ | 0.82 | 527 | 0.0052 | 0.24 | 1.72 |

Table 2 Factors and their levels on PSS simulations

| Level \ Factor | A(h) | B($R_p$) | C($L_1$) | D($L_2$) |
|---|---|---|---|---|
| 1 | 0 | 5 | 70 | 70 |
| 2 | 3 | 6 | 71 | 70 |
| 3 | 6 | 7 | 72 | 70 |

Table 3 Results of matrix experiment along the $L_9$ orthogonal array

| Exp. No. | A | B | C | D | $LPH_{ca}$ | $\Delta\varepsilon_1$ | $\eta$ |
|---|---|---|---|---|---|---|---|
| 1 | 1 | 1 | 1 | 1 | 30.3 | 0.1000 | 20 |
| 2 | 1 | 2 | 2 | 1 | 29.5 | 0.0500 | 26.02 |
| 3 | 1 | 3 | 3 | 1 | 29.6 | 0.0700 | 23.1 |
| 4 | 2 | 1 | 2 | 1 | 29.2 | 0.0100 | 40 |
| 5 | 2 | 2 | 3 | 1 | 29.1 | 0.0015 | 56.5 |
| 6 | 2 | 3 | 1 | 1 | 29.4 | 0.0150 | 36.5 |
| 7 | 3 | 1 | 3 | 1 | 28 | 0.0700 | 23.1 |
| 8 | 3 | 2 | 2 | 1 | 28.2 | 0.0600 | 28.2 |
| 9 | 3 | 3 | 1 | 1 | 28.1 | 0.0700 | 28 |

Table 4 ANOM and ANOVA table for the PSS test simulation

| Factor | Average $\eta$ by level(dB) | | | Degree of freedom | Sum of squares | Mean square | F ratio |
|---|---|---|---|---|---|---|---|
| | 1 | 2 | 3 | | | | |
| A | 23.04 | **44.3**[a] | 26.43 | 2 | 782.8 | 391.4 | 11.15 |
| B | 27.7 | **36.91**[a] | 29.2 | 2 | 157.9 | 78.95 | |
| C | 28.16 | 31.41 | **34.2**[a] | 2 | 54.83[b] | 27.4 | |
| D | | | | | | | |
| Error | | | | 0 | | | |
| Total | | | | 6 | 995.53 | | |
| Pooled error | | | | (2) | (54.83) | (27.4) | |

(1) Overall mean of $\eta$ is 31.26 dB.

(2) [a]Indicate the optimum level

(3) [b]Indicate the sum-of-squares added together to estimate the pooled error sum of squares, shown in parentheses.

(4) The F ratio is calculated by using the pooled error mean square